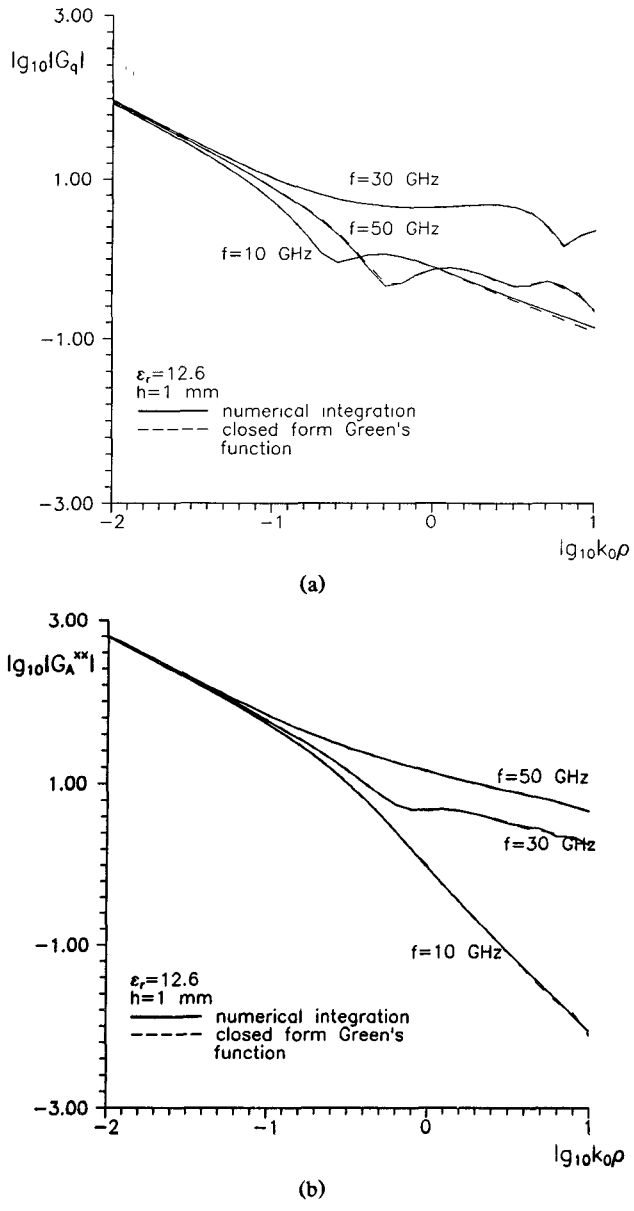

Fig. 4. (a) The amplitude of the scalar potential G_q. (b) The amplitude of the vector potential G_A^{xx}.

quasi-dynamic images (i.e., eq. (10)), three terms for the complex images (i.e., Table I), and two terms for the surface waves. The savings in computer time can be more than tenfold, with the error less than 1% compared with the numerical integration of the Sommerfeld integrals.

Finally, it should be pointed out that the closed-form equation (18) applies to all source-to-field distances on the substrate surface. As discussed in the Introduction, it is in the form $A + B + C$, representing the contributions of the quasi-dynamic images, the complex images, and the surface wave. At different distances, certain contributions may be small and can be dropped without causing much error in the spatial Green's function.

Acknowledgment

The authors thank the reviewers for many constructive comments.

References

[1] Y. L. Chow, "An approximate dynamic spatial Green's function in three dimensions for finite length microstrip lines," *IEEE Trans. Microwave Theory Tech.*, vol. MTT-28, pp. 393–397, 1980.
[2] J. R. Mosig and F. E. Gardiol, "A dynamical radiation model for microstrip structures," in *Advances in Electronics and Electron Physics*, vol. 59. London: Academic Press, 1982, pp. 139–239.
[3] P. B. Katehi and N. G. Alexopolous, "Real axis integration of Sommerfeld integrals with application to printed circuit antennas," *J. Math. Phys.*, vol. 24, pp. 527–533, 1983.
[4] E. Alanen and I. V. Lindell, "Exact image method for field calculation in horizontally layered medium above a conducting ground plane," *Proc. Inst. Elec. Eng.*, vol. 133, pt.H, pp. 297–304, 1986.
[5] D. G. Fang, J. J. Yang, and G. Y. Delisle, "Discrete image theory for horizontal electric dipoles in a multilayered medium," *Proc. Inst. Elec. Eng.*, vol. 135, pt. H, pp. 297–303, 1988.
[6] J. A. Stratton, *Electromagnetic Theory*. New York: McGraw-Hill, 1941, p. 576, eq. (17).
[7] J. Dai and Y. L. Chow, "A reduced model of a series of image charges for study MMIC's," in *Proc. Second Asia-Pacific Microwave Conf.* (Beijing, China), Oct. 26–28, 1988.
[8] J. Duncan, *The Elements of Complex Analysis*. New York: Wiley, 1968.
[9] R. W. Hamming, *Numerical Methods for Scientists and Engineers*. New York: Dover, 1973, pp. 620–622.

Measurement of Dielectric Constant Using a Microstrip Ring Resonator

P. A. Bernard and J. M. Gautray

Abstract —**A new approach for measuring the permittivity of dielectric materials by means of a microstrip ring resonator is presented. The method is used in conjunction with the variational calculation of the line capacitance of a multilayer microstriplike transmission line to compute the effective permittivity and hence the resonant frequency of the ring. The results are compared with measurements made in *X*-band waveguide cavity by cavity perturbation techniques.**

I. Introduction

Microstrip ring resonators are frequently employed in microwave integrated circuit design. Resonant structures such as rectangular, circular, and ring resonators have been widely studied in oscillators and filters [1]–[4]. The resonator is a large ring that is several wavelengths long to avoid mutual inductance effects [5] and problems caused by end effects in rectangular microstrip resonators. What is more, these ring resonators have Q factors of about 250, compared with 100 for rectangular ones.

The method presented here is based on the fact that the effective permittivity will change if the alumina/air boundary is modified by placing a dielectric material above the alumina substrate, thereby changing the resonant frequency of the ring. The variational calculation of the line capacitance [6], [7] is used to compute the effective permittivity of the multilayer microstriplike ring resonator and hence the resonant frequency for several test materials.

It is well known that the dielectric constant varies with frequency. Since we are very concerned with this frequency dependence, the test material above the Al_2O_3 substrate must be

Manuscript received February 5, 1990; revised July 9, 1990.
The authors are with the Universite de Bordeaux I, U.E.R. De Physique, Laboratoire De Physique Experimentale et Des Micro-Ondes, 351, Cours de la Liberation, 33405 Talence Cedex, France.
IEEE Log Number 9041947.

0018-9480/91/0300-0592$01.00 ©1991 IEEE

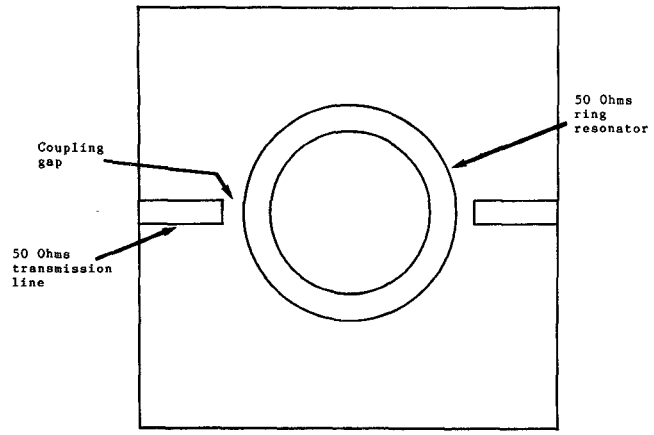

Fig. 1. Plan view of microstrip ring resonator.

sufficiently thin in order to obtain a new resonant frequency that is as close as possible to the resonant frequency of the ring without the test material. These results are compared with measurements made in an X-band waveguide cavity using perturbation theory [8]. A cylindrical rod is cut from the test material and inserted in the middle of a TE_{10} cavity, where the electric field is maximum. In the particular case where the dielectric rod crosses the cavity, the dielectric constant of the test material is simply related to resonant frequency drift.

This study has a double purpose: the first is to show that microelectronics technology can be directly used to build microwave measurement applicators easily and at low cost; the second is to show that the plates of the dielectric samples under test do not require prior machining.

II. Microstrip Ring Resonator

The ring resonator is a large ring with a mean diameter of 9.36 mm (Fig. 1). The measured resonant frequencies are approximately given by

$$F_a = 1.32n \text{ GHz} \tag{1}$$

where n is the harmonic number. F_1, the fundamental resonant frequency, is equal to 1.32 GHz. A more accurate relation can be obtained by taking into account the dispersion occurring in the Al_2O_3 substrate.

Owens [9], [10] has derived accurate equations from Wheeler's works [11], [12] for calculating the quasi-static effective permittivity, ϵ_{r0}. The effective permittivity at a given frequency, denoted ϵ_{rf}, is then computed knowing the substrate thickness and the characteristic impedance of the line. The resonance frequency of the ring can thus be calculated from the more accurate equation

$$\pi d_m = n\lambda_g = \frac{n\lambda_0}{\sqrt{\epsilon_{rf}}} \tag{2}$$

where d_m is the mean diameter of the ring. On the other hand, measurement of a resonant frequency of the ring with a known diameter makes it possible to compute ϵ_{rf} at that frequency provided the fundamental resonant frequency is known.

III. The Multilayer Microstriplike Transmission Line

The resonant frequency drift in the resonator shown in Fig. 2 must be as small as possible. For this reason the test material must be thinner for materials having larger dielectric constants. The PTFE (polytetrafluoro-ethylene) block situated above the test material is used to get rid of the air trapped between the substrate and the test material by firm pressing. The line capacitance of an unloaded line ($\epsilon_1 = \epsilon_2 = \epsilon_3 = 1$) is C_0 while the line capacitance of a loaded line is denoted C. The relation between the wavelength of the unloaded line, λ_0, and that of the loaded line, λ, is given by

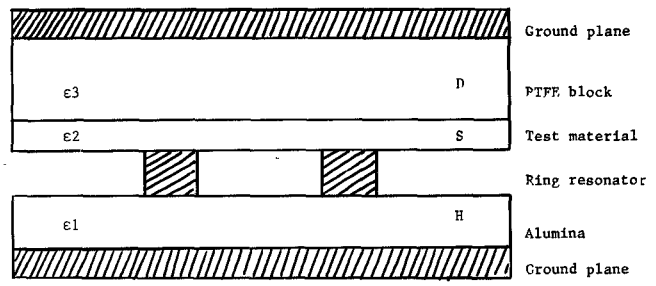

Fig. 2. Side view of resonator etched on alumina substrate. H denotes substrate thickness, S test material thickness, and D PTFE thickness. Not to scale. ϵ_1, ϵ_2, and ϵ_3 are respectively the dielectric constants of alumina, test material, and PTFE.

$$\lambda = \left(\frac{C_0}{C}\right)^{1/2} \lambda_0. \tag{3}$$

For nonmagnetic materials, (3) can be written

$$\lambda = \frac{\lambda_0}{\sqrt{\epsilon_{rf}}}. \tag{4}$$

A program has been computed and ϵ_{rf} is directly obtained from the preliminary calculations of C_0 and C:

$$\frac{\lambda}{\lambda_0} = \left(\frac{C_0}{C}\right)^{1/2} = \left(\frac{1}{\epsilon_{rf}}\right)^{1/2} \tag{5}$$

$$C = C_0 \epsilon_{rf}. \tag{6}$$

The line thickness is considered negligible, and the air trapped between the substrate and the test material is ignored. The variational expression of the line capacitance in the β coordinate is given by Yamashita [6], [7]:

$$\frac{1}{C} = \frac{1}{\pi Q^2 \epsilon_0} \int_0^\infty [f(\beta)]^2 g(\beta)\, d\beta \tag{7}$$

where

$$Q \equiv \int_{-\infty}^{+\infty} f(x)\, dx \tag{8}$$

in the x coordinate. The quantity $f(\beta)$, the charge density distribution, is the Fourier transform of $f(x)$ and is given by

$$f(\beta) = \int_{-\infty}^{+\infty} f(x) e^{j\beta x} dx. \tag{9}$$

For the three-layer microstriplike line, $g(\beta)$ is equal to

$$g(\beta) = \frac{\epsilon_3 d + \epsilon_2 s}{|\beta|\{\epsilon_3 d[\epsilon_1 h + \epsilon_2 s] + \epsilon_2[\epsilon_2 + \epsilon_1 hs]\}} \tag{10}$$

where

$$h = \coth(|\beta| H) \tag{11}$$

$$d = \coth(|\beta| D) \tag{12}$$

$$s = \coth(|\beta| S). \tag{13}$$

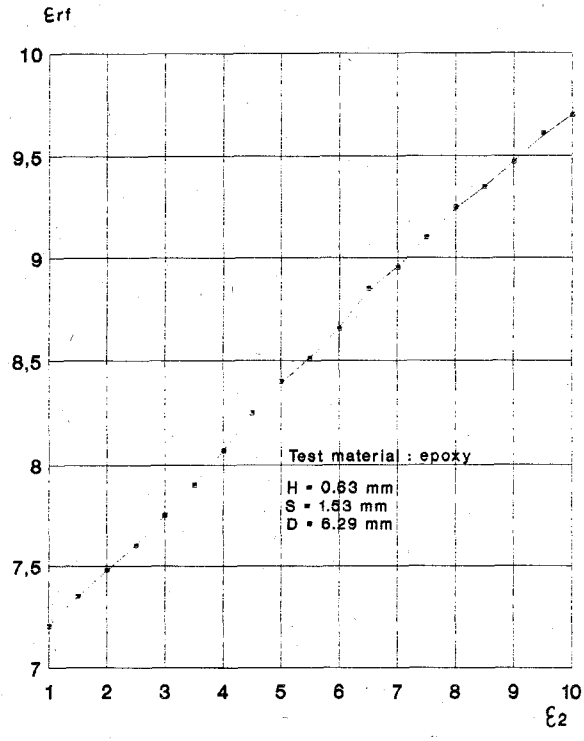

Fig. 3. Graph of ϵ_{rf} versus ϵ_2.

The function $f(x)$ is approximated by the trial function

$$f(x) = \begin{cases} 1+\left(\dfrac{2x}{\omega}\right)^3, & -\dfrac{\omega}{2} \leqslant x \leqslant \dfrac{\omega}{2} \\ 0, & \text{otherwise} \end{cases} \tag{14}$$

ω being the width of the line. The Fourier transform of $f(x)$, $f(\beta)$, is given by

$$\frac{1}{Q} f(\beta) = \frac{8}{5}\left\{\frac{\sin(\beta\omega/2)}{\beta\omega/2}\right\} + \frac{12}{5(\beta\omega/2)^2} \cdot \left\{\cos(\beta\omega/2) - 2\frac{\sin(\beta\omega/2)}{\beta\omega/2} + \frac{\sin^2(\beta\omega/4)}{(\beta\omega/4)^2}\right\}. \tag{15}$$

Equations (7) and (10)–(14) are used to compute C_0 by substituting $\epsilon_1 = \epsilon_2 = \epsilon_3 = 1$. C is obtained by making $\epsilon_1 = 10$ (alumina) and $\epsilon_3 = 2$ (PTFE), with ϵ_2 the dielectric constant of the test material. For different values of ϵ_2, we plot the variation of ϵ_{rf} with ϵ_2 when H, S, and D are given (Fig. 3).

The resonant frequencies of the ring with and without the test material are measured. They are called respectively F_1 and F_0. The effective permittivity without the test material, ϵ_{rf0}, is readily obtained by making $\epsilon_1 = 10$, $\epsilon_2 = \epsilon_3 = 1$, and D, $S \to \infty$. The effective permittivity in the presence of the test material, ϵ_{rf1}, is then calculated from (2):

$$\pi d_m = \frac{n\lambda_0}{\sqrt{\epsilon_{rf}}} = \frac{nv_0}{F_0\sqrt{\epsilon_{rf0}}} = \frac{nv_0}{F_1\sqrt{\epsilon_{rf1}}} \tag{16}$$

where v_0 is the velocity of light. Hence

$$\epsilon_{rf1} = \epsilon_{rf0}\left(\frac{F_0}{F_1}\right)^2. \tag{17}$$

Knowing ϵ_{rf1}, we can search for ϵ_2 from the curve given in Fig. 3. For epoxy ϵ_{rf1} was equal to 8.09, giving a corresponding value of $\epsilon_2 = 4.0$. This result must be confirmed by measuring the dielectric constant of epoxy in a waveguide using the well-known cavity perturbation technique.

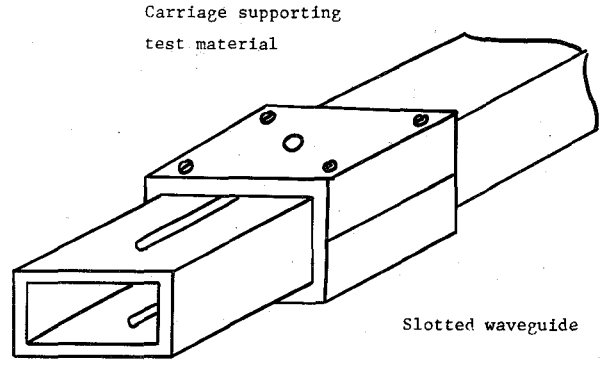

Fig. 4. Rectangular cavity with sliding fixture to support rod-shaped test material.

IV. Dielectric Measurement in a Waveguide Cavity

The waveguide cavity is a TE_{10} mode supporter with a coupling iris at one end and a mobile short circuit at the other, in order to modify the resonant frequency of the cavity (Fig. 4). Test material cut in the form of a long cylindrical rod and supported on the carriage is then placed in the maximum electric field region. In the particular case where the test material crosses the cavity, we have a simple expression for the dielectric constant of the material [13]:

$$\frac{F_0 - F_1}{F_0} = Kv(\epsilon - 1) \tag{18}$$

where K is the filling factor of the cavity, v is the volume of the test material inside the cavity, ϵ is the dielectric constant of the test material, F_0 is the resonant frequency of unloaded cavity, and F_1 is the resonant frequency of loaded cavity. The filling factor, K, is obtained experimentally with a material of known dielectric constant. For instance, PTFE has a dielectric constant which is nearly equal to 2 in the X band. If the resonant frequency of the cavity loaded with PTFE is called F_p, then

$$K = \frac{1}{v_p}\frac{F_0 - F_p}{F_0} \tag{19}$$

where v_p is the volume of PTFE.

V. Results and Conclusions

A block diagram of the configuration retained for measuring the resonant frequency of the ring is shown in Fig. 5. When the ring is replaced by the cavity device, reflected power is obtained at port 3 of the circulator. Several plastic materials were cut for measurements with the ring resonator and the same materials, in the form of rods, were mounted in the cavity for comparative measurements. The resonant frequency of the cavity was tuned to be equal to that of the ring.

The results are given in Table I. Here ϵ_R represents results obtained with the microstrip ring, and ϵ_C results obtained with the cavity. The resonant frequency of both the ring and the cavity resonator was 11.5 GHz.

These results tend to confirm that microstrip resonators can be used for dielectric measurements. However, for materials having large dielectric constants ($\epsilon_r = 10$), comparative results seem to diverge rapidly. This is explained by the fact that the cavity perturbation method is limited to materials having low dielectric constants. For large-dielectric-constant materials, the

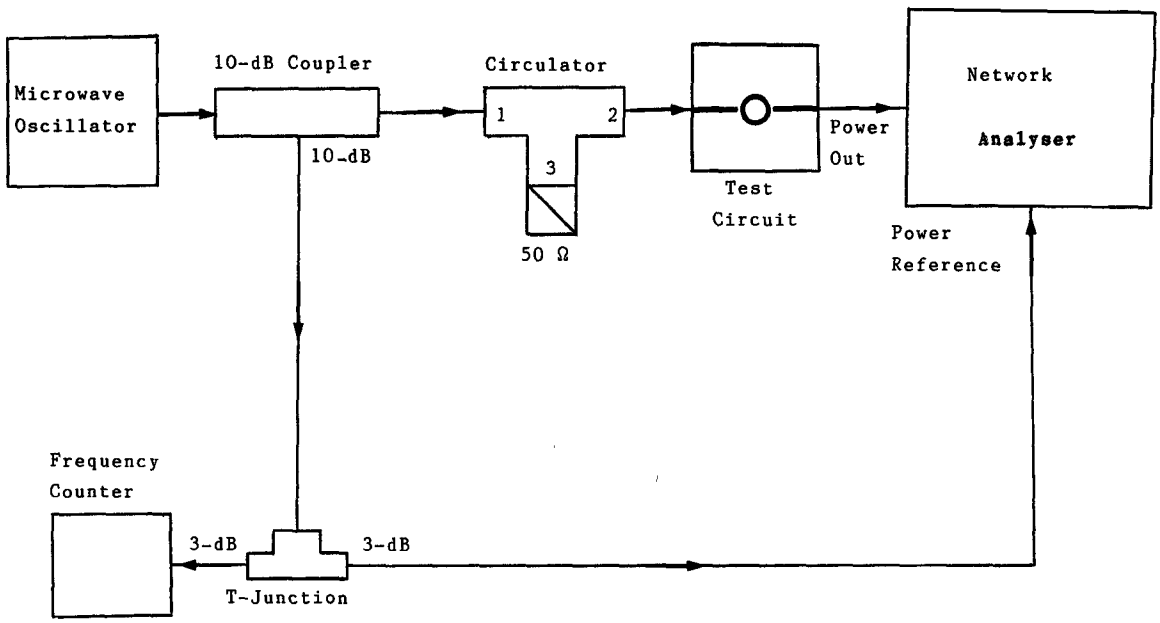

Fig. 5. Resonant frequency measurement setup.

TABLE I

Test Material	ϵ_R	ϵ_C
A	4.0	3.9
	4.0	3.8
	4.2	3.9
B	8.0	9.0
	8.5	9.3
C	2.3	2.2
	2.2	2.3
D	2.8	2.6
	3.2	3.0
	2.8	3.2
E	2.9	2.5
	2.7	2.5
F	7.8	9.3

All measurements were made at 11.5 GHz (unloaded resonant frequency).

frequency drift is a constant and the proportionality rule given by (18) is no longer respected.

Compared with other, more time consuming measurement methods, this method makes it possible to save time and is well suited to material characterization for industrial applications.

References

[1] S. Mao, S. Jones, and G. D. Vendelin, "Millimeter-wave integrated circuits," *IEEE Trans. Microwave Theory Tech.*, vol. MTT-16, pp. 455–461, July 1968.

[2] G. D'inzeo, F. Giannini, C. M. Sodi, and R. Sorrentino, "Method of analysis and filtering properties of microwave planar networks," *IEEE Trans. Microwave Theory Tech.*, vol. MTT-26, pp. 462–471, July 1978.

[3] J. Watkins, "Circular resonant structures in microstrip," *Electron. Lett.*, vol. 5, no. 21, pp. 524–525, Oct. 16, 1969.

[4] T. Itoh and R. Mittra, "A new method for calculating the capacitance of a circular disk for microwave integrated circuits," *IEEE Trans. Microwave Theory Tech.*, vol. MTT-21, pp. 431–432, June 1973.

[5] P. Troughton, "Measurement techniques in microstrip," *Electron. Lett.*, vol. 5, no. 2, pp. 25–26, Jan. 23, 1969.

[6] E. Yamashita and R. Mittra, "Variational method for the analysis of microstrip lines," *IEEE Trans. Microwave Theory Tech.*, vol. MTT-16, pp. 251–256, Apr. 1968.

[7] E. Yamashita, "Variational method for the analysis of microstrip-like transmission lines," *IEEE Trans. Microwave Theory Tech.*, vol. MTT-16, pp. 529–535, Aug. 1968.

[8] R. A. Waldron, "Perturbation theory of resonant cavities," Inst. Electric Engineers, Monograph no. 373E, Apr. 1960.

[9] R. P. Owens, "Accurate analytical determination of quasi-static microstrip line parameters," *Radio Electron. Eng.*, vol. 46, no. 7, pp. 360–364, July 1976.

[10] T. C. Edwards and R. P. Owens, "2–18 GHz dispersions measurements on 10–100 ohm microstrip lines on sapphire," *IEEE Trans. Microwave Theory Tech.*, vol. MTT-24, pp. 506–513, Aug. 1976.

[11] H. A. Wheeler, "Transmission-line properties of parallel wide strips by a conformal mapping approximation," *IEEE Trans. Microwave Theory Tech.*, vol. MTT-12, pp. 280–289, May 1964.

[12] H. A. Wheeler, "Transmission-line properties of parallel strips separated by a dielectric sheet," *IEEE Trans. Microwave Theory Tech.*, vol. MTT-13, pp. 172–185, Mar. 1965.

[13] J. C. Anderson, *Dielectrics*. London: Chapman and Hall, 1964.

Characterization of Microstrip Open End in the Structure of a Parallel-Coupled Stripline Resonator Filter

Tomoki Uwano

Abstract—**This paper describes an accurate characterization of stripline open end in the parallel-coupled microstrip filter configuration. The method of analysis is based on a two-port resonance technique where the spectral-domain approach is used as a full-wave analysis. Even- and odd-mode edge effects are characterized separately by solving transcendental equations. Calculated results are used for the design of certain filters and the experimental results show excellent filter performances, which validates this method and leads to accurate filter design in practice.**

Manuscript received June 12, 1990; revised October 29, 1990.

The author is with the Image Technology Research Laboratory, Matsushita Electric Industrial Company Ltd., 1006 Oaza-kadoma, Osaka 571, Japan.

IEEE Log Number 9041960.

0018-9480/91/0300-0595$01.00 ©1991 IEEE